

Change Detection for Sustainable Redevelopment of AI Identified Brownfields from Satellite Imagery using Statistical and Clustering Techniques - A Case Study on Supply Chain Location Analysis

Konrad Dürrbeck
Fraunhofer IIS
konrad.duerrbeck@iis.fraunhofer.de

Kiran Gollapalli
Fraunhofer IIS
sai.kiran.srivatsav.gollapalli@iis.fraunhofer.de

Daniel Reich
Fraunhofer IIS
daniel.reich@iis.fraunhofer.de

Uwe Veres-Homm
Fraunhofer IIS
uwe.veres-homm@iis.fraunhofer.de

Md Obaidullah Sk
Fraunhofer IIS
sk.obaidullah@gmail.com

Roland Fischer
Fraunhofer IIS
roland.fischer@iis.fraunhofer.de

Abstract

In the area of Supply Chain Network Design and Location Analysis, it is critical to find an optimal geographic location for production and logistics with a desired area size, usually a large piece of land near the industrial estates or urban settlements, to develop it into a distribution center or a warehouse etc. The reasons may include ease of access to the potential end customers or other business partners for vertical integration of their supply chains. Considering United Nations Sustainable Development Goal 11 and other existing urban planning regulations, it may not always be feasible to locate a suitable greenfield site. One approach to address this problem is by identifying the existing brownfields using high resolution satellite and aerial images. A Machine Learning(ML)-based image classification algorithm is being developed which can make a classification on all available land parcels into brownfields or other active sites with the help of these high resolution images. However, these high resolution images are expensive and difficult to be frequently collected. An economically affordable alternative are more frequently available low resolution images which can be used to validate the classification with an appropriate change detection method. This paper introduces a detailed method for detecting changes in brownfield sites. The process includes initial classification with DOP21 (high resolution digital orthophoto captured around 2021) imagery, enhancement using SPOT21 and SPOT23 (Satellite pour l'Observation de la Terre) images for low resolution analysis and a series of steps. The experimental outcome shows the effectiveness of the proposed method to distinguish physical changes within the areas of interest, demonstrating substantive applicability in large-scale analysis.

Keywords: Sustainability, Change Detection, Land Use Classification, Brownfield Analysis, Supply Chain Location Analysis.

1. Introduction

Location decisions of facilities in the supply chain are one part of the network design of a complex supply chain network Govindan and Fattahi (2017). Furthermore, the selection of this location in the specific supply chain network is decided based on various criteria. These criteria could include both economic, as well as social and environmental factors Y. He et al. (2017). Regarding the environmental criteria, the ecological impact on the landscape (Bouhana and Chafai (2013), Guo et al. (2015), Y. He et al. (2017)) should also be considered in the planning phase of a location of the logistic center when designing supply chain networks. As per the United Nations Sustainable Development Goal we need to consider the interests of future generations in relation to urbanization and sustainable urban planning (SDGs 11.6, 11.7, 11.a and 11.b) United Nations Sustainable Development Group (UNSDG) (2024). The work we present here is in support of the goal of the United Nations.

In such a context discussed above, locating a parcel of land (usually a greenfield) that can be developed into the desired facility might not always be available. Even if available, developing it might not be most sustainable approach. With the existing urban planning regulation and in respect of the UNSDG goal 11, it is recommended to first consider the redevelopment of existing brownfields before developing greenfields. Many governments are also showing interest when preparing a digital land data base for future use. Typically a brownfield, which is also known as a

”redevelopment site” is a type of land which was used previously for commercial or industrial development purposes but is currently in an abandoned stage. Brownfield identification has a direct link with the sustainable development of modern societies across the world. The primary challenge with this recommendation is to identify the existing brownfields, which are tightly weaved through the urban and industrial settlements. Traditional approaches for brownfield identification used GIS (Geographic Information System) to inspect satellite images and locating such regions based on certain predefined characteristics. Expert intervention was necessary for such a type of characterization. Nowadays, researchers are exploring the possibilities of AI-based (Artificial Intelligence) based techniques for brownfield detection using satellite images. But this task requires several post-processing stages to receive the expected results. Given that high resolution images often are not up to date, an AI-based prediction might mark a location as a brownfield (figure 1.b) while it became a construction site since the image was captured (figure 1.a) rendering the result incorrect. Using high resolution coverage from 2022 of the same parcel, the robustness of the trained model is noteworthy as it identified it as a construction site with a probability 0.81, while the brownfield probability is just 0.02. It’s important to note that high resolution image coverage from 2022 is not readily available due to economical and practical limitations. Interestingly, it is possible to detect these changes with the help of low resolution SPOT images collected in 2023 (figure 1.c) and 2021 (figure 1.d). Low resolution panchromatic images like these are not suitable for a precise classification using the above AI as they do not offer enough detail. To address this issue and to make our AI-based classification system more resilient, another post-processing technique could be the application of further change detection algorithms on those identified brownfields. With previous models, the classification results were seen as the final outcome but the new method follows up the classification with a series of post-processing change detection techniques. This shows that there is a pressing need to develop robust change detection techniques for a better AI-based automated land cover classification system.

In remote sensing and GIS, change detection is a useful strategy to find discrepancies in two satellite images of the same parcel captured at different times. Change detection algorithms compare the spatial representation of two image points in varying time and measure the differences in the variables of interest. Typical applications of change detection are observing the consequences of flooding, forest fires, continuous droughts, other natural calamities and weather extremity

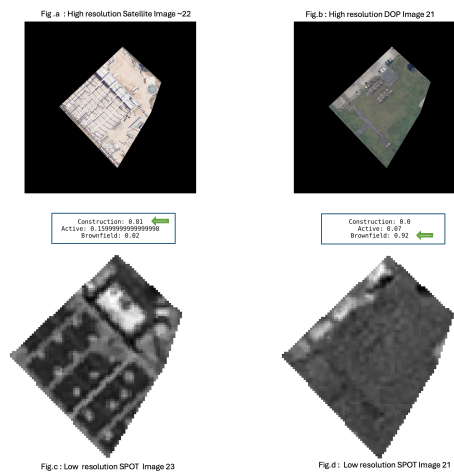


Figure 1. Sample high resolution RGB image and low resolution panchromatic images of the same site.

conditions. In addition, the application of change detection techniques is being used in the area of sustainable development such as brownfield analysis.

1.1. Review

With the use of machine learning methods this paper contributes to the development of digital supply chain services (Pflaum et al. (2019), Farajpour et al. (2022)). The present work strengthens digital supply chain services by providing effective identification of brownfields from satellite image data. The role of location analysis is very crucial in the supply chain management. Finding the optimal location for new business or extending existing business is very important for any company. Our work will bridge the gap by finding suitable locations in accordance with governmental land redevelopment policies. In literature several works can be found on brownfield analysis such as Maliene et al. (2012), Dürbeck et al. (2022) to name a few. Among the available publications on change detection, an unsupervised iterative method based on the expectation-maximization algorithm was proposed by Bruzzone and Prieto (2000) during in 2000. Huo et al. (2016) reported a supervised change detection approach based on relationship learning. Bovolo and Bruzzone (2008) proposed an unsupervised change detection technique from multi-spectral remote-sensing images based on similarity measures and semi-supervised SVM (Support Vector Machine). A random forest based fusion of SAR (Synthetic Aperture Radar) and multi-spectral images was done by Seo et al. (2018) to overcome the insufficiency of single remote sensing data in change detection. Xie et al. (2016)

proposed a hierarchical decision tree based change detection from high resolution remote sensing images. To obtain the image object a fractal net evolution approach was used followed by optimal scales of different objects determined by an evaluation index based on the accuracy of the classification, which in turn creates the feature space. Then a hierarchical decision tree was applied onto multi-temporal high resolution remote sensing images. Lastly, the change detection was determined by comparing the multi-temporal classification results. Cao et al. (2014) proposed a change detection method using high resolution SPOT5 remote sensing images by combining pixel-level and object-level components followed by a SVM based classification. Hao et al. (2014) proposed an unsupervised expectation-maximization based level set method for change detection. The used Gaussian mixture model and expectation-maximization together were used to compute mean values of changed and unchanged pixels in the difference image. A land-use decision support in brownfield redevelopment for urban renewal based on crowd sourced data has been proposed by Liu et al. (2019). In another work, Hao et al. (2020) proposed a superpixel-based markov random field model for unsupervised change detection. A few other related works on change detection were also proposed in Zhou et al. (2016) Touati et al. (2020). Deep learning based techniques are very popular tools nowadays, which also applies in the domain of change detection. Some of the interesting CNN based works on change detection are mentioned in Zhan et al. (2017) R. Huang et al. (2021) Hou et al. (2020). An extreme machine learning based change detection method was proposed in Khurana et al. (2020).

The above mentioned methods show a considerable performance for some specific image types during specific applications. For our brownfield project we were using satellite and aerial images from sources like Google and Bing which can be of varying age. That is why the use of the change detection algorithm was inevitable to observe the changes over time in a particular location. In present work, we have used statistical techniques to compute various parameters directly on the image data, which make the method computationally faster. The following cluster analysis was done on the computed statistical values. We summarize our key contributions as follows:

1. A novel change detection method using statistical and clustering based techniques is proposed for brownfield detection in areas of Germany.
2. We have implemented the method using satellite image data of classified brownfields and received

encouraging results.

3. The proposed method computes some statistical parameters of images, which then are used for cluster analysis, resulting computation improvements compared to traditional learning based approaches.
4. Present work facilitates the problem of supply chain location analysis by accurate identification and an attempt of validation of identified brownfields.

1.2. Change Detection in Brownfield Analysis

The most important question which arises is when to use change detection in an application. Figure 2 shows an overall architecture of the brownfield identification. At first, input images are provided to the system, followed by some pre-processing steps such as gray-scale conversion, thresholding, contour detection, largest contour identification, bounding rectangle fitting and ROI (Region Of Interest) extraction. Once the pre-processing is done, the images are then passed through an active learning loop. In short, active learning is a machine learning approach where the model can interactively query a user to label new data points. This is useful in situations where labeled data is not readily available. We have used three pre-trained deep learning models namely ResNet by K. He et al. (2015), VGG-19 by Simonyan and Zisserman (2015), DenseNet121 by G. Huang et al. (2018), InceptionResNetV2 by Szegedy et al. (2016) and one in-house developed custom CNN model which we called EcoBrownfieldNet for classification of brownfields. Among all, the best predictive model is chosen and the result is then fed to the change detection module. For our change detection algorithm, we have taken low resolution panchromatic SPOT images covering most of Germany, for both 2021 and 2023, and already classified high resolution brownfield images of the same areas which were last updated in 2021. We then compared the low resolution image pairs taken at different points in time. The final outcome belongs to one of the two categories i.e. "Change" or "No Change". If we found the outcome to indicate that there was no change, the earlier prediction based on the high resolution coverage will be used as the final result. If the outcome is showing a significant change on the other hand, we invalidate the previous prediction as the location may not be a valid brownfield anymore.

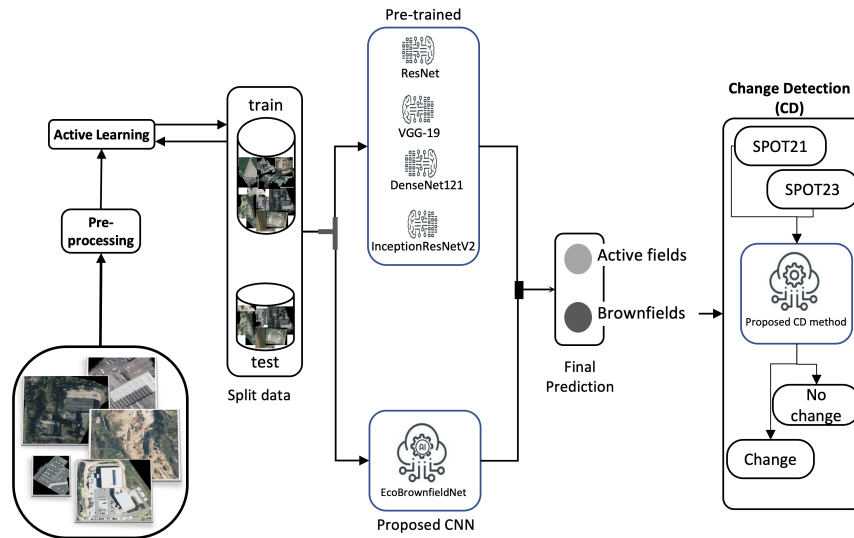


Figure 2. Flow diagram of the overall brownfield analysis architecture including change detection.

2. Methodology

This involves a series of steps including image collection, computation of statistical metrics, normalization, dimensionality reduction, clustering and cluster investigation. In the following subsections we will be discussing them one by one.

2.1. Image Collection

The process of collecting SPOT21 and SPOT23 images, each with a 1.5m ground resolution, for specified areas marked by polygons. In total 75,077 images had to be compared in order to find which pair of images exhibit a structural change such as a solar park or a new building making the previous prediction on high resolution images invalid. Here, one needs to be aware that the low resolution panchromatic images that are taken in 2021 differ from 2023 due to various reasons such as different sensors in the satellites, environmental and lighting conditions. Figure 3 is an example of the SPOT images.

Here the high resolution google image which was captured during 2021 and was classified as brownfield and the SPOT image captured during same period show that our current trained model is able to classify these images as brownfields. The SPOT23 image shows a completely finished building a potentially active business, which makes this site no longer a brownfield. And as the model doesn't have a more current high resolution image due to practical and economical limitations, this method serves the purpose to establish preliminary information about the current

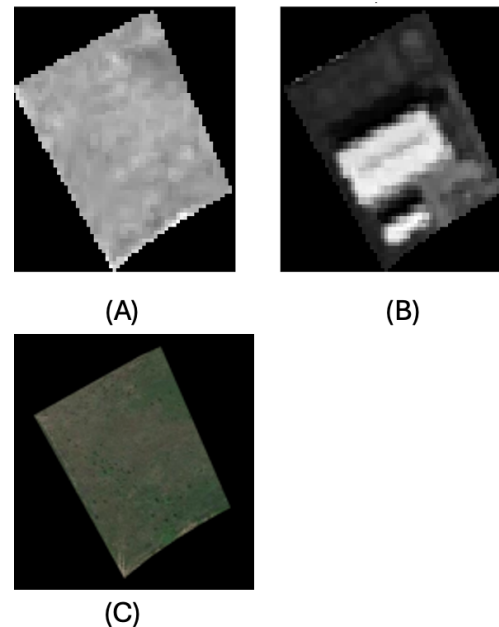


Figure 3. Sample low resolution (A), (B) and high resolution (C) images.

state and can be used as a lead to prioritise for which areas satellite coverage should be tasked.

2.2. Metric Calculation

The primary focus of this work is to propose a faster and robust method for change detection by utilizing statistical parameters that assess image correlation.

After a series of experiments on images of several locations, we selected four key metrics: mean squared error (MSE), peak signal-to-noise ratio (PSNR), error relative global dimensionless synthesis (ERGAS), and visual information fidelity (VIF). Though there were a few other metrics such as Universal Quality Image Index (UQI), Spatial Correlation Coefficient (SCC), Relative Average Spectral Error (RASE), and Spectral Angle Mapper (SAM). We decided on the previous mentioned four metrics because of their experimental effectiveness. A short definition is provided below for each of the used parameters.

MSE – It is the deviation of an estimator which measures the average of the squares of the errors—that being, the average squared difference between the estimated values and the actual value.

PSNR – It is the ratio between the maximum possible power of a signal and the power of corrupting noise that affects the fidelity of its representation.

ERGAS – A more advanced image quality index than RMSE. ERGAS is a global statistic expressing the quality of the enhanced resolution image. ERGAS measures the transition between spatial and spectral information.

VIF – The visual information fidelity (VIF) has an interesting feature: it can capture the effects of linear contrast enhancements on images, and quantify the improvement in visual quality. A VIF value greater than unity indicates this improvement, while a VIF value less than unity signifies a loss of visual quality.

2.3. Normalization and Dimensionality Reduction

The above discussed metrics are calculated on the 75,077 image pairs (SPOT21 and SPOT23) which are clipped using the same polygon that the high resolution image were based on which were classified as brownfields. The values obtained in these steps are shown in table 1. Afterwards, we applied a data normalization technique to keep all the values within the range of 0 to 1. This normalization step is important because in the later stage, we will first be using the dimensionality reduction, distance and kernel density based clustering algorithms, which needs range bound data. The results before and after normalization process are given in table 1 and 2.

After normalization, we applied the dimensionality reduction using principal component analysis (PCA) Jolliffe and Cadima (2016). PCA is a technique used to reduce the dimensionality of such data sets, increasing interpretability while minimizing information loss. It does this by creating new uncorrelated variables that

Stats	MSE	PSNR	ERGAS	VIF
count	75077	75077	75077	75077
mean	1.6e5	1.8	3.5e2	0.218
std	6.9e5	6.652	8.5e3	0.068
min	6	-28.758	30	3e-6
25%	1.4e5	-2.486	151	0.169
50%	3.7e4	2.415	220	0.215
75%	1.1e5	6.653	341	0.263
max	4.8e7	40.429	1.8e6	0.588

Table 1. Metrics before applying normalization

Stats	MSE	PSNR	ERGAS	VIF
count	75077	75077	75077	75077
mean	0.003	0.443	0.00017	0.370
std	0.014	0.096	0.0045	0.115
min	0.000	0.000	0.000	0.000
25%	0.000288	0.380	0.000064	0.288
50%	0.000763	0.451	0.00010	0.365
75%	0.002360	0.512	0.000165	0.447
max	1.000	1.000	1.000	1.000

Table 2. Metrics after applying normalization

successively maximize the variance. Finding such new variables, the principal components, boils down to solving the eigenvalue / eigenvector problem, and the new variables are defined by the existing data set, not a priori, making PCA an adaptive data analysis technique. In the next step, we applied clustering algorithm on those principal components followed by detailed cluster analysis.

2.4. Unsupervised Clustering

The two principal components are then utilised as an input for K means clustering algorithm. The optimal number of clusters in this case was determined to be four after an iterative process of testing with 2, 3, 6, and 8 clusters. During each iteration, a random sample of 10 images was drawn multiple times from each cluster. Based on this process, three out of the four clusters consistently showed no desired change, while one cluster exhibited a high degree of desired change. Here desired change refers to the location being no longer a brownfield. Following figure 4 shows the outcome of K-Means clustering technique.

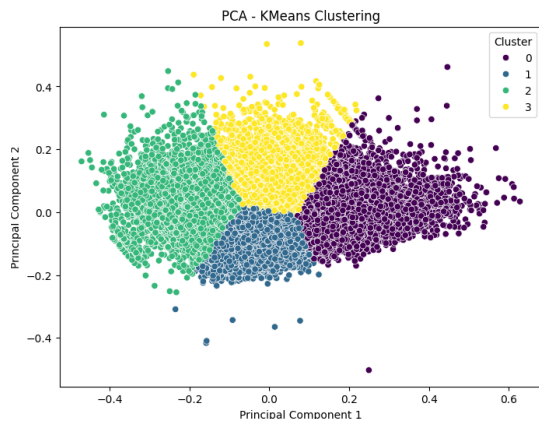


Figure 4. Outcome after applying K Means clustering technique

	Count	Decision
Cluster 0	23346	No change
Cluster 1	17969	No change
Cluster 2	16906	change
Cluster 3	16856	No change
Sum	75077	

Table 3. Summary of Clusters and Decisions for Dataset Analysis

3. Experiments

3.1. Experimental setup

Our experimental setup for the classification of brownfields using aerial imagery was built on a system with 16 GB of RAM and an Apple M2 Pro processor. We conducted our experiments on a stable platform running macOS Sonoma 14.5. For developing and evaluating our methods, we employed pytorch version 1.13.0 as our deep learning method for the classification of brownfields.

3.2. Dataset

We did our experiments on 75,077 image pairs, i.e. SPOT21 and SPOT23 images. The whole dataset was available in the tag image file format (TIFF). Following figure 5 and 6 shows a sample pair of SPOT21 and SPOT23 images. In figure 5 SPOT21(A) and SPOT23(B) images are similar and no changes can be observed. In figure 6 SPOT21(A) and SPOT23(B) images are completely different and changes can be observed, in this case due to the presence of a solar panel.

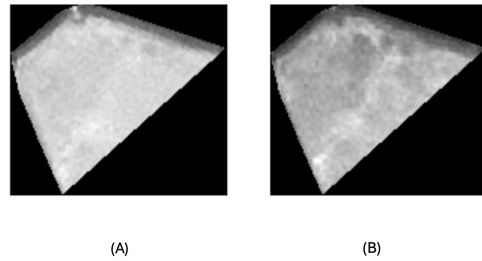


Figure 5. sample image pair_1 of SPOT21(A) and SPOT23(B)

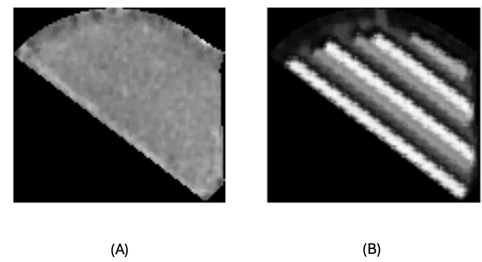


Figure 6. sample image pair_2 of SPOT21(A) and SPOT23(B)

4. Results and Discussion

4.1. Results

Detailed examination of each cluster by analyzing 250 randomly selected examples each to ensure thorough investigation with the help of human annotations. The human annotator is answering the question whether two SPOT images have a change or not by selecting "agree", "disagree" or "can't decide". Here, "agree" means there is a change between two images, "disagree" means there is no change between two images, "can't decide" means there is no concrete decision as one of the image could have a bit of cloud coverage referring to figure 7 or some other noise.

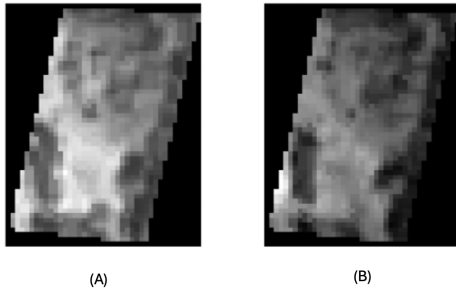


Figure 7. Sample images showing probable cloud coverage

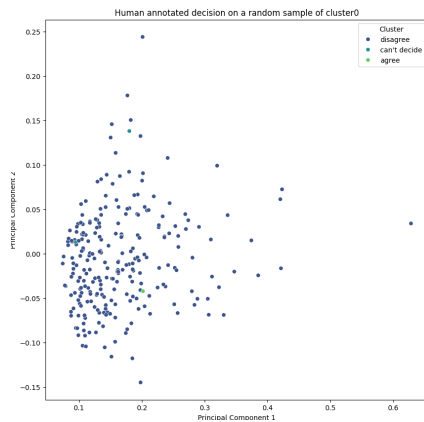


Figure 8. Distribution of brownfields in Cluster 0

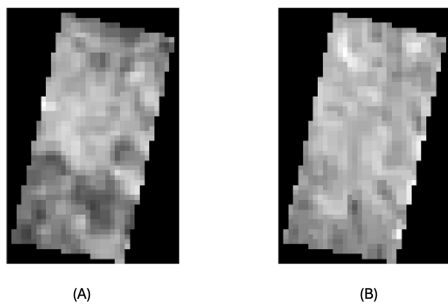


Figure 9. Sample panchromatic images from Cluster 0 for the year 2021(A) and 2023(B)

Figure 8 presents a scatter plot with a random sample of 250 points that are manually annotated for cluster 0. Samples of such images are shown in figure 9. A majority of the points are densely packed around the origin, indicating a high concentration of data in the central region. A large proportion of the sample points (247/250 which translates to 98.8% accuracy) are labeled as "disagree" (black) against the question

of whether there is a change, which is inline with the decision for this cluster. In contrast, the labels "can't decide" (green) and "agree" (light black) are sparsely distributed, highlighting areas of uncertainty within the cluster.

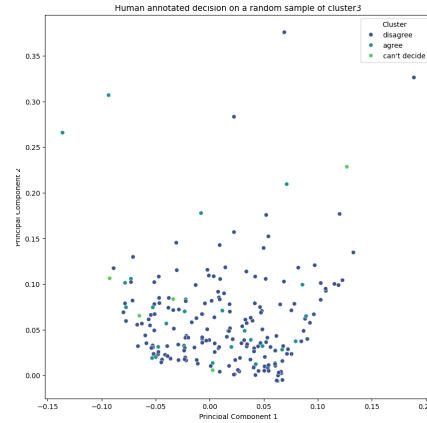


Figure 10. Distribution of brownfields in Cluster 3

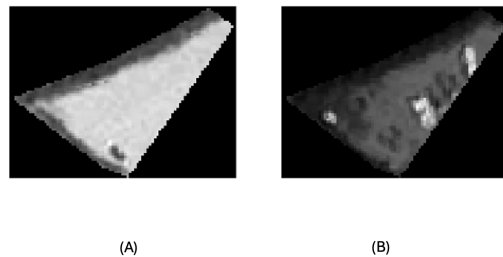


Figure 11. Sample panchromatic images from Cluster 3 for the year 2021(A) and 2023(B)

Figure 10 presents a scatter plot with a random sample of 250 points that are manually annotated for cluster 3. Samples of such images are shown in figure 11. The majority of the points are densely packed around the origin, indicating a high concentration of data in the central region. A large proportion of the sample points (210/250 which translates to 84% accuracy) are labeled as "disagree" (black) against the question of whether there is a change, which aligns with the decision. In contrast, the labels "can't decide" (green) and "agree" (light black) for change are sparsely distributed, highlighting areas of uncertainty within the cluster.

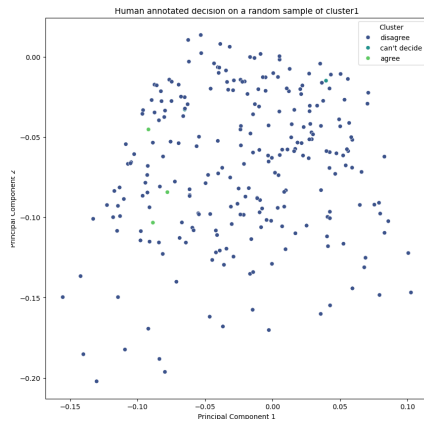


Figure 12. Distribution of brownfields in Cluster 1

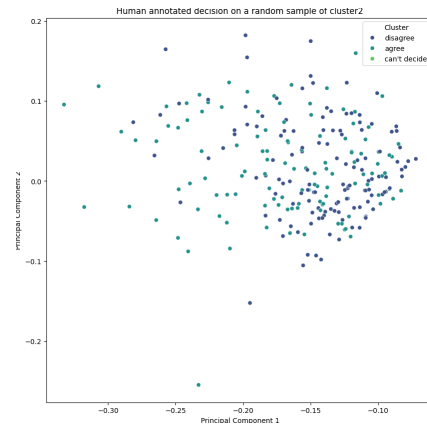


Figure 14. Distribution of brownfields in Cluster 2

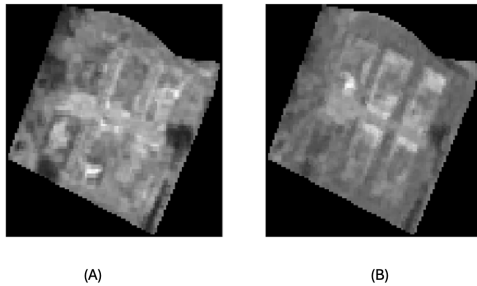


Figure 13. Sample panchromatic images from Cluster 1 for the year 2021(A) and 2023(B)

Figure 12 presents a scatter plot with a random sample of 250 points from cluster 1. Samples of such images are shown in figure 13. The majority of the points are spread across the plot without a dense concentration around the origin, suggesting a distributed presence of data points in the central region. The points are color-coded based on human annotations into three categories: "disagree" (black), "agree" (green), and "can't decide" (light black). The plot reveals that a large proportion of the sample points (245/250 which translates to 98% accuracy) are labeled as "disagree". In contrast, the labels "agree" for change and "can't decide" are sparsely distributed, highlighting fewer areas of uncertainty within the cluster.

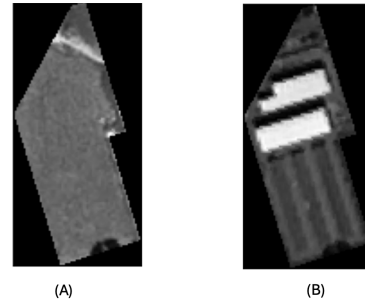


Figure 15. Sample panchromatic images from Cluster 2 for the year 2021(A) and 2023(B)

The scatter plot depicted in figure 14 illustrates a human-annotated random sample of 250 points from cluster 2. Each point in the plot is colored according to the annotation categories: "disagree" (black), "agree" (light green), and "can't decide" (green). Samples of such images is shown in figure 15. There is no clear distinction within this cluster between decision of "agree" and "disagree". The plot reveals that nearly half the points (140/250 which translates to 56% accuracy) are labelled as "disagree" against the question of whether there is a change, which aligns with the decision for this cluster that there is high possibility to find the desired changes.

The overall accuracy of this method when investigated using 1000 sample points is at 84%.

4.2. Discussion

The effectiveness of the proposed method outperform human experts in terms of decision making time for the whole dataset of 75,000 pairs of images while maintaining a comparable accuracy level. The aim of this solution is to solve a specific

problem with the supply chain location analysis, thus the generalization ability of this solution is not being prioritized.

5. Conclusions and Future Scope

For business optimization (Perez et al. (2021)), supply chain location analysis is a very important topic of discussion nowadays. Be it finding locations for new or expanding existing businesses, the prerequisite is finding suitable land. In this paper, we propose a change detection method for brownfield analysis using satellite imagery. We have taken low resolution panchromatic images which are available for both the years 2021 and 2023 of previously classified brownfields based on high resolution images. The majority of these high resolution images covering most of Germany were last updated in 2021. Then compared both of the low resolution images using our algorithm. The experiment was conducted over 75,000 pair of satellite images which were classified as brownfield, and after inspection on a random sample of 250 for each cluster, a satisfactory outcome was found. The method is faster compared to traditional machine learning based approaches as it directly computes the statistical parameters on the image data followed by a cluster investigation. In traditional learning based approaches we need to feed lot of labelled images to train the model which requires much more time.

A more current high resolution image is not available to be used with the model due to practical and economical limitations. This method serves the purpose to establish preliminary information about the current state and can be used as a lead to acquire up to date image coverage from satellite image providers only for locations where a change has been detected. In addition, the method is currently tested over different regions of Germany. There is a scope to implement the same for other geographic locations as well. This will help for a ready to go supply chain location analysis solution for the brownfield redevelopment problem for digital land map generation.

In addition, mathematical optimization can be used to determine optimal locations in networks that allow access to markets and customers. The availability of land is one of the most important location factors for large new commercial settlements. The already acute shortage of land in some conurbations, together with the EU-level target of a steady reduction in net new land sealing (net zero by 2050 in Germany), means that the reactivation of unused or derelict commercial areas is the only way to actually achieve an optimal location from a mathematical point of view. The future

consideration of brownfields that are currently safely available will enable logistics network planning to find optimal locations even beyond the next few years.

6. Acknowledgement

The work is supported by ERCIM post-doctoral fellowship.

References

- Bouhana, A., & Chafai, H. (2013). A multi-criteria decision making approach based on fuzzy theory and fuzzy preference relations for urban distribution centers' location selection under uncertain environments. *Proceedings of the International Conference on Advanced Logistics and Transport*, 556–561.
- Bovolo, F., & Bruzzone, L. (2008). A novel approach to unsupervised change detection based on a semisupervised svm and a similarity measure. *IEEE Trans. Geosci. Remote. Sens.*, (46(7)), 2070–2082.
- Bruzzone, L., & Prieto, D. F. (2000). Automatic analysis of the difference image for unsupervised change detection. *IEEE Trans. Geosci. Remote. Sens.*, (38(3)), 1171–1182.
- Cao, G., Du, P., He, X., & Zhang, Z. (2014). Automatic change detection in high-resolution remote-sensing images by means of level set evolution and support vector machine classification. *International Journal of Remote Sensing*, (35(16)), 6255–6270.
- Dürbeck, K., Frey, T., & Müller, S. (2022). Automatic extraction of brownfield sites from aerial images using neural networks. In: *Land Use Monitoring XIV, Contributions to Land Management, Data, Methods and Analysis*, 305–314.
- Farajpour, F., Zegordi, S. H., & Niknam, R. (2022). Digital supply chain blueprint via a systematic literature review. *Technological Forecasting and Social Change*, 184. <https://doi.org/doi.org/10.1016/j.techfore.2022.121976>
- Govindan, K., & Fattahi, M. (2017). Supply chain network design under uncertainty: A comprehensive review and future research directions. *European Journal of Operational Research*, 263(1), 108–141. <https://doi.org/10.1016/j.ejor.2017.04.009>
- Guo, S., Zhao, H., Gu, F., Wang, W., & Li, H. (2015). Optimal site selection of electric vehicle charging station by using fuzzy topsis based

- on sustainability perspective. *Applied Energy*, 158, 390–402. <https://doi.org/10.1016/j.apenergy.2015.08.082>
- Hao, M., Du, P., & Zhang, L. (2014). Unsupervised change detection with expectation-maximization-based level set. *IEEE Geosci. Remote. Sens. Lett.*, (11(1)), 210–214.
- Hao, M., Zhang, L., & Du, P. (2020). An advanced superpixel-based markov random field model for unsupervised change detection. *IEEE Geosci. Remote. Sens. Lett.*, (17(8)), 1401–1405.
- He, K., Zhang, X., Ren, S., & Sun, J. (2015). Deep residual learning for image recognition.
- He, Y., Wang, L., & Wang, Z. (2017). Sustainable decision making for joint distribution center location choice. *Transportation Research Part D: Transport and Environment*, 55, 202–216. <https://doi.org/10.1016/j.trd.2017.07.001>
- Hou, B., Zhang, L., Xie, Z., & Wang, Z. (2020). From w-net to cdgan: Bitemporal change detection via deep learning techniques. *IEEE Trans. Geosci. Remote. Sens.*, (58(3)), 1790–1802.
- Huang, G., Liu, Z., Van Der Maaten, L., & Weinberger, K. Q. (2018). Densely connected convolutional networks.
- Huang, R., Zhang, L., Li, X., & Ma, Y. (2021). Change detection with various combinations of fluid pyramid integration networks. *IEEE Geosci. Remote. Sens. Lett.*, (437), 84–94.
- Huo, C., Zhan, Y., & Zhang, L. (2016). Learning relationship for very high resolution image change detection. *IEEE J. Sel. Top. Appl. Earth Obs. Remote. Sens.*, (9(8)), 3384–3394.
- Jolliffe, I. T., & Cadima, J. (2016). Principal component analysis: A review and recent developments. *Philos Trans A Math Phys Eng Sci.*, (374(2065)), 20150202.
- Khurana, M., Bhattacharya, A., & Mohan, C. K. (2020). A unified approach to change detection using an adaptive ensemble of extreme learning machines. *IEEE Geosci. Remote. Sens. Lett.*, (17(5)), 794–798.
- Liu, Y., Wu, Q., Chen, L., & Zhang, H. (2019). Land-use decision support in brownfield redevelopment for urban renewal based on crowdsourced data and a presence-and-background learning (pbl) method. *Land Use Policy*, 88, Article 104188. <https://doi.org/10.1016/j.landusepol.2019.104188>
- Maliene, V., Malys, N., & Maliene, N. (2012). Brownfield regeneration: Waterfront site developments in liverpool and cologne. *Journal of Environmental Engineering and Landscape Management*, 20(1), 5–16. <https://doi.org/10.3846/16486897.2012.659030>
- Perez, H., Ortega, J., & Martinez, A. (2021). Optimization of extended business processes in digital supply chains using mathematical programming. *Computers Chemical Engineering*, 152. <https://doi.org/10.1016/j.compchemeng.2021.107323>
- Pflaum, A., Bodendorf, F., Chen, X., & Thamm, T. (2019). The digital supply chain of the future: From drivers to technologies and applications. <https://api.semanticscholar.org/CorpusID:86464506>
- Seo, D., Kim, J., & Park, S. (2018). Fusion of sar and multispectral images using random forest regression for change detection. *ISPRS Int. J. Geo Inf.*, (7(10)), 401.
- Simonyan, K., & Zisserman, A. (2015). Very deep convolutional networks for large-scale image recognition.
- Szegedy, C., Ioffe, S., Vanhoucke, V., & Alemi, A. (2016). Inception-v4, inception-resnet and the impact of residual connections on learning.
- Touati, R., Chaabane, F., Alaya, B., & Bouhleb, M. S. (2020). Multimodal change detection in remote sensing images using an unsupervised pixel pairwise based markov random field model. *IEEE Trans. Image Process.*, (29), 757–767.
- United Nations Sustainable Development Group (UNSDG). (2024). *Sustainable development goals* [Accessed: 2024-06-14]. <https://www.un.org/en/common-agenda/sustainable-development-goals>
- Xie, Z., Zhang, X., & Li, S. (2016). Hierarchical decision tree for change detection using high resolution remote sensing images. *Geoinformatics in Sustainable Ecosystem and Society, ser. Communications in Computer and Information Science*, (980), 176–184.
- Zhan, Y., Huo, C., Zhang, L., & Chen, P. (2017). Change detection based on deep siamese convolutional network for optical aerial images. *IEEE Geosci. Remote. Sens. Lett.*, (14(10)), 1845–1849.
- Zhou, L., Li, W., Zhang, L., & Du, Q. (2016). Change detection based on conditional random field with region connection constraints in high-resolution remote sensing images. *IEEE J. Sel. Top. Appl. Earth Obs. Remote. Sens.*, (9(8)), 3478–3488.